Journal of Structural Geology, Vol. 15, No. 9/10, pp. 1207 to 1222, 1993
Printed in Great Britain

0191-8141/93 $06.00+0.00
Pergamon Press Ltd

High-pressure deformation of calcite marble and its transformation to aragonite under non-hydrostatic conditions

BRADLEY R. HACKER

Department of Geology, Stanford University, Stanford, CA 94305-2115, U.S.A.

and

STEPHEN H. KIRBY

U.S. Geological Survey, Menlo Park, CA 94205, U.S.A.

(*Received* 17 *July* 1992; *accepted in revised form* 18 *March* 1993)

Abstract—We conducted deformation experiments on Carrara marble in the aragonite and calcite stability fields to observe the synkinematic transformation of calcite to aragonite, and to identify any relationships between transformation and deformation or sample strength. Deformation-induced microstructures in calcite crystals varied most significantly with temperature, ranging from limited slip and twinning at 400°C, limited recrystallization at 500°C, widespread recrystallization at 600 and 700°C, to grain growth at 800–900°C. Variations in confining pressure from 0.3 to 2.0 GPa have no apparent effect on calcite deformation microstructures. Aragonite grew in 10^{-6}–10^{-7} s^{-1} strain rate tests conducted for 18–524 h at confining pressures of 1.7–2.0 GPa and temperatures of 500–600°C. As in our previously reported hydrostatic experiments on this same transformation, the aragonite nucleated on calcite grain boundaries. The extent of transformation varied from a few percent conversion near pistons at 400°C, 2.0 GPa and 10^{-4} s^{-1} strain rate in a 0.8 h long experiment, to 98% transformation in a 21-day test at a strain rate of 10^{-7} s^{-1}, a temperature of 600°C and a pressure of 2.0 GPa. At 500°C, porphyroblastic 100–200 μm aragonite crystals grew at a rate faster than 8×10^{-10} m s^{-1}. At 600°C, the growth of aragonite neoblasts was slower, $\sim 6 \times 10^{-11}$ m s^{-1}, and formed 'glove-and-finger' cellular-precipitation-like textures identical to those observed in hydrostatic experiments. The transformation to aragonite is not accompanied by a shear instability or anisotropic aragonite growth, consistent with its relatively small volume change and latent heat in comparison with compounds that do display those features.

INTRODUCTION

MARBLE has long been considered one of the geologic materials whose rheology is best understood. It was among the first geologic materials investigated for its inelastic properties (Adams & Nicholson 1901, von Kármán 1911). A number of milestones in understanding the rheology of rock-forming minerals have been achieved with calcite marble: the first extensive study of the brittle–ductile transition (Heard 1960), the first comprehensive study of the rheology of dislocation creep (Heard 1963, Heard & Raleigh 1972), the first comprehensive study of the effects of mineral preferred orientation on rheology and plasticity (Griggs & Miller 1961), and the first experimental indication of superplastic creep (Schmid *et al.* 1977). At low temperatures and pressures, marble deforms by brittle faulting, cataclasis and mechanical twinning. Increasing pressure causes increased ductility, and increasing temperature leads to ductile dislocation creep (e.g. Heard, 1963). All these deformation regimes are easily accessible within the laboratory.

The calcite↔aragonite transformation may be the most extensively investigated polymorphic phase transition in geology (see, for example, Johannes & Puhan 1971). For powders and single crystals, the reaction rates and mechanism have been well characterized (e.g. Brar & Schloessin 1979, Carlson & Rosenfeld 1981, Snow & Yund 1987). Recent progress has been made toward understanding the calcite→aragonite transformation in fully dense marble (Hacker *et al.* 1992). Because these fundamental aspects of calcite deformation and of the equilibrium phase relations under hydrostatic conditions are reasonably well understood, the calcite→aragonite transformation is especially attractive for learning how stress and deformation affect phase transformation and how phase transformations can affect material rheology and deformation microstructures.

Griggs *et al* (1960) reported reconnaissance high-pressure shear experiments on calcite marble at a temperature of 500°C, crossing the calcite–aragonite equilibrium pressure numerous times at high rates of deformation. Stable shearing was always observed in those experiments, a point emphasized later by Griggs & Baker (1969) and Griggs (1972). An exploratory study by Wenk *et al.* (1973) on Solnhofen limestone revealed that calcite can be transformed to aragonite during conventional triaxial deformation experiments at temperatures of 300–800°C, confining pressures of 1.0–2.2 GPa and strain rates of 10^{-4}–10^{-7} s^{-1}. That experimental program, directed toward studying preferred orientations, was limited by large temperature, pressure and stress gradients in their samples. Snow & Yund (1987) recently showed that stress and deformation accelerate the transformation of single crystal calcite to aragonite.

They found that complete transformation occurred during 25% shortening at a strain rate of 10^{-6} s^{-1}, a confining pressure of 1.5 GPa and a temperature of 500°C, whereas a second sample treated hydrostatically at the same pressure and temperature showed only 5% transformation. Gillet *et al.* (1987) also performed calcite→aragonite experiments at 1.3 GPa, 500°C and 10^{-4} s^{-1} strain rate. With transmission electron microscopy (TEM), they observed aragonite domains growing into the host calcite crystals and, at least locally, topotactic growth of aragonite on calcite. The lack of a systematic suite of deformation experiments on polycrystalline calcite under well-controlled conditions spanning the calcite–aragonite equilibrium boundary prompted us to make a more complete study of this transformation. This study addresses the questions: how do stress and deformation affect the transformation rate and mechanism; how does the transformation affect the mechanical behavior of the samples; and does Carrara marble transform to aragonite differently from Solnholfen limestone (experiments of Wenk *et al.* 1973)?

EXPERIMENTAL PROCEDURE

Starting material

The starting material is nominally Carrara marble, obtained from a monument company (see Fig. 3a). The only impurities present above optical spectroscopy detection limits (generally 5 ppm) are: 0.36% MgO, 0.02% FeO, 130 ppm Sr and 49 ppm MnO. No phases other than calcite were detected by X-ray powder diffraction, petrographic inspection or transmission-electron microscopy. The grain size measured in thin section by the method of mean linear intercepts is 78 μm, notably finer grained than the Carrara marble with 200 μm size grains used in previous studies by Rutter (1972, 1974) and Schmid *et al.* (1980). There is no shape preferred orientation and no lattice preferred orientation. Most grains contain twins spaced ~25 μm apart. The calcite crystals possess weak undulatory extinction, and a few have low-angle subgrain boundaries that trend generally subperpendicular to the twins. Grain boundaries are non-planar, indicating that this marble has not reached textural equilibrium. Transmission-electron microscopy reveals a rather uniform distribution of 10^{12}–10^{13} dislocations per square meter. About one-third are unit dislocations, whereas the remainder are in tangles. Loops and curved segments of dislocations are abundant.

Experimental apparatus

Each sample was cored from a block of Carrara marble, dried overnight under vacuum at 175°C, placed inside a 0.125 mm thick cylindrical silver jacket previously annealed at 875°C, and separated from the 90% Al_2O_3·10% TiO_2 load pistons by 0.025 mm thick silver shims. Experiments at confining pressures of up to 2.0 GPa were conducted in a single, piston-cylinder, solid-pressure-medium rock-deformation apparatus (Griggs 1967) at the U.S. Geological Survey. The samples were cylinders 6.22 mm in diameter and ~15 mm in length. Aside from the sample, jacket, end pieces and furnace, the entire assembly was composed of NaCl. Temperature was provided by resistive heating of a cylindrical, uniform thickness graphite furnace surrounding the sample, and was measured by one Pt–$Pt_{90}Rh_{10}$ thermocouple touching the exterior of the sample jacket near the midpoint of the sample long axis. Temperature control was precise to ± 1°C. At 400°C, the center of the sample was ~60°C warmer than the ends (Kronenberg *et al.* 1990). Temperatures were not corrected for pressure or differential stress effects on the thermocouple e.m.f., and the reported confining pressure was not corrected for friction within the assembly or the strength of the confining medium. We used 3.2 mm diameter load pistons to reduce piston friction and ensure that the stress was measured as precisely as possible.

Stress measurements in solid-medium deformation apparatus are inaccurate. We performed calibration experiments on polycrystalline halite samples at 25°C and 400°C, 0.5–1.5 GPa, and 10^{-4} s^{-1} strain rate, using our standard experimental set-up. At 400°C, about one-half of the apparent sample strength is related to frictional and viscous losses in our high pressure cell—regardless of confining pressure. At higher temperatures and slower strain rates, the frictional contribution is expected to be less. There have been no *in situ* pressure calibrations for our NaCl cell in the Griggs deformation apparatus. However, Mirwald *et al.* (1975) conducted melting experiments on pure metals and LiCl in a similar NaCl cell in hydrostatic apparatus over a temperature range of 300–1400°C using the DTA method. They found that melting point temperatures showed insignificant hysteresis during pressure cycling and corresponded closely to melting curves obtained from truly hydrostatic gas apparatus. They estimated the absolute accuracy of their pressure measurements as ± (1% + 0.05 GPa). In the absence of a pressure calibration of a NaCl cell in the Griggs apparatus, we adopt Mirwald *et al.*'s (1975) estimate of the uncertainty of pressure.

Low-pressure (0.1–0.7 GPa) experiments were conducted in an argon-pressure-medium Heard-type rock-deformation apparatus at the U.S. Geological Survey (Kronenberg *et al.* 1990). The samples were right circular cylinders, 8.9 mm in diameter and ~20 mm in length. Temperature was provided by resistive heating of a platinum furnace and was measured by one Pt–$Pt_{90}Rh_{10}$ thermocouple touching a tungsten carbide spacer at one end of the sample. At 400°C, the center of the sample was ~8°C warmer than the ends (Kronenberg *et al.* 1990). Temperature was controlled to ± 5°C for most experiments. Confining pressure was maintained to within 0.5 MPa by a servo-controlled pump. The strain rate was controlled by a servo-controlled stepping motor and the axial load was measured with an internal load

cell of the Heard type (within the pressure vessel). Sample strengths are accurate to within 10 MPa.

Experimental output from the displacement transducers, force gauge, pressure gauge and thermocouple of both types of apparatus, was monitored and reduced to values of differential stress, pressure, strain and time on a HP-85 computer. Strains and strain rates were calculated from two displacement transducers after correction for apparatus distortion produced by the applied load. The differential stress was calculated as the difference between the axial normal stress, σ_1, and the confining pressure, σ_3, and corrected for changes in sample diameter during deformation. The volume reduction accompanying aragonite formation means that the calculated stresses for transformed samples are underestimated.

Analytical methods

After each experiment, the sample was sawed in half lengthwise. One doubly polished ~20 μm thin section of every sample was made for examination by optical microscopy. The extent of transformation was determined by examining 400 points with an automated point-counting stage on an optical microscope. The aragonite growth rate was also determined with an optical microscope. In samples containing subequant neoblasts of aragonite, the growth rate was determined by measuring the half-width of the largest aragonite neoblasts; smaller neoblasts were assumed to be the result of the thin section not passing through the center of the crystal. For samples containing aragonite along calcite–calcite grain boundaries, the growth rate was determined by measuring the half-width of aragonite separating once-adjacent calcite grains. Measurements were made only in areas where the calcite 'fingers' (see below) were subparallel to the plane of the thin section—to ensure that the rate measured was not an apparent rate of interface migration. Additional doubly polished <30 μm sections of selected samples were made and thin foils prepared for transmission electron microscopy (TEM) by argon ion milling. A Philips 400 scanning/transmission electron microscope at Stanford, equipped with a double-tilt goniometer stage, was used for phase identification and to characterize microstructures.

RESULTS

The conditions of the deformation experiments span temperatures of 400–900°C, and strain rates of 10^{-7}–10^{-4} s^{-1} (Fig. 1 and the Appendix). Nominal confining pressures, P, ranged from 0.1 to 2.0 GPa. Differential stress, σ, was as high as 660 MPa, and thus the mean stress, $\bar{\sigma} = P + \sigma/3$, was within ~0.2 GPa of the imposed confining pressure. As outlined above, sample strengths may be overestimated by a factor of 2, and thus the mean stresses were probably within 0.1 GPa of the imposed confining pressure.

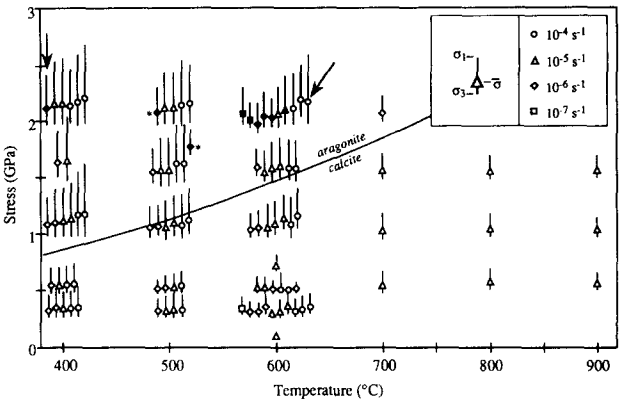

Fig. 1. Pressure–temperature–strain rate conditions of the experiments. Samples that contained widely distributed aragonite are shown with filled symbols; open symbols indicate no aragonite. Arrows point to the samples in which aragonite developed only in one corner of the sample near the piston and asterisks identify samples with porphyroblastic aragonite. The dot for each sample shows the nominal mean stress and the vertical bar denotes the limits of the nominal normal stresses, which range from the applied load (σ_1) to the confining pressure (σ_3). Experiments at each pressure and temperature have been spaced arbitrarily about the true temperature so that the different symbols are visible. Uncertainties of pressures and stresses discussed in the text are not shown. Equilibrium boundary below 550°C from Johannes & Puhan (1971); above 550°C from unpublished work by S. R. Bohlen, W. B. Hankins and B. R. Hacker.

Mechanical data

Most stress–strain curves show relatively linear elastic loading, yielding, and then flow at a reasonably constant differential stress (Fig. 2). Strain hardening is exhibited by some samples tested at 400°C and confining pressures of 0.3–0.5 GPa. The hardening is apparently inhibited by increased pressure and temperature, although this may be an artifact of the use of gas apparatus at low pressures and use of solid-medium apparatus at high pressures. Rowe & Rutter (1990) also noted a change from strain-hardening at 400°C to steady-state flow at higher temperatures in Carrara marble experimentally deformed at 0.1 GPa confining pressure. At conditions within the calcite stability field, the stress supported by samples increases with increasing strain rate and decreasing temperature in the manner characteristic of rocks deforming by ductile dislocation creep. Samples containing aragonite are not systematically stronger or weaker than samples in which aragonite did not form. A detailed analysis of the mechanical behavior and sample microstructures will be published in a separate paper.

Deformation and recrystallization microstructures

The principal intracrystalline deformation mechanisms of calcite are slip on $r\{10\bar{1}4\}$, $f\{\bar{1}012\}$, $c\{0001\}$ and $a\{\bar{1}2\bar{1}0\}$, and twinning on $e\{\bar{1}018\}$ and $r\{10\bar{1}4\}$ (Wenk 1985). At low temperatures, twinning is easier than r slip, which dominates at 400–650°C (Weiss & Turner 1972), whereas f slip dominates between 500 and 800°C (Griggs *et al.* 1960, Casey *et al.* 1978, Friedman & Higgs 1981). These transitions depend on strain rate and grain size as well as temperature, with a change of ~100°C roughly equivalent to a change in strain rate of six

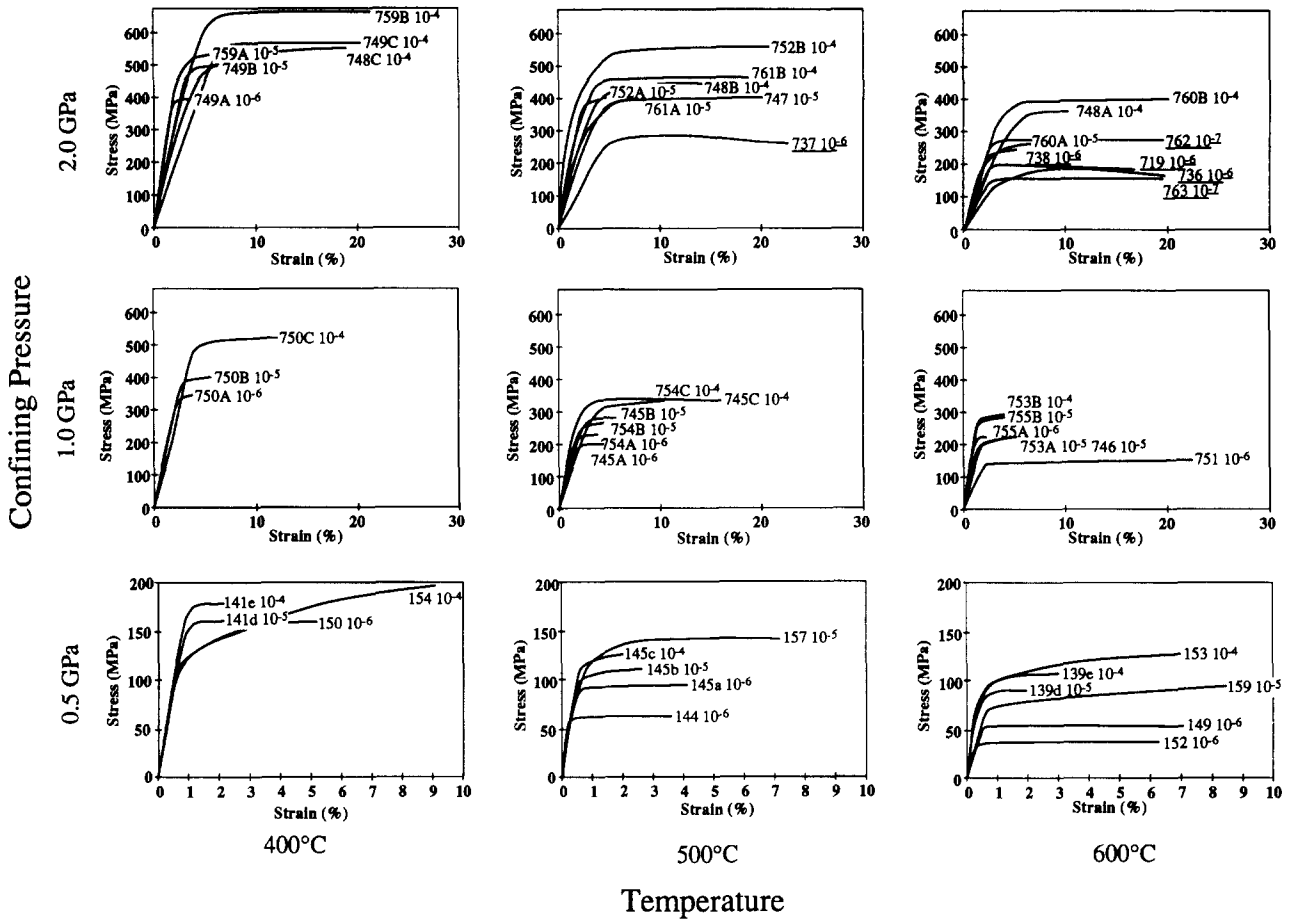

Fig. 2. Representative stress–strain curves for Carrara marble. Each curve is labeled with the experiment number and strain rate (s^{-1}). Experiments performed at pressures ≥1.0 GPa were conducted in solid-medium apparatus and those at lower pressures were completed in gas-medium apparatus. Underlines indicate those experiments in which aragonite formed throughout the sample. Experiments at 0.3, 1.5 and 1.7 GPa confining pressure (Table 1) are not shown.

decades (Ferreira & Turner 1964). Because the maximum shortening that can be achieved by complete *e* twinning is theoretically 29%, and perhaps nearer 15% in polycrystalline marble (Wenk 1985), any additional shortening must take place by other means such as dislocation glide or recrystallization.

Optical microscopy and TEM observations of our deformed marble samples reveal distinct microstructural changes with increasing temperature (Fig. 3). We have not found changes in microstructure that can be correlated with the apparent strength increase at higher pressures (Fig. 4).

At 400°C and all strain rates, virtually all the deformation occurred by mechanical twinning (Fig. 3b), in accord with earlier studies on Carrara marble (e.g. Rutter 1974, Casey *et al.* 1978). The microstructures are similar to those described for 'Regime 1' of Carrara marble deformation by Schmid *et al.* (1980)—although their samples were deformed at higher temperatures (600–700°C) and generally faster strain rates (10^{-3}–10^{-5} s^{-1}), and were coarser grained (200 μm). Most calcite grains are highly twinned, with twin boundaries spaced every 1–8 μm, and most twin boundaries are oriented at high angles to the compression direction. Fewer grains have two or more sets of widely spaced twins that are inclined ~30–50° to the compression axis. The twinning and slip produced variably inequant grain shapes with axial ratios ranging up to about 2:1 in the most deformed samples. Recrystallization is either absent or minor in these samples.

The microstructures developed at 500°C are independent of strain rate from 10^{-6} to 10^{-4} s^{-1}, and similar to those developed at 400°C. Most samples contain twins and undulatory extinction without recrystallization, as observed by Rutter (1974) in similar experiments to 12% strain at 0.15 GPa confining pressure. Two samples contain ≤ 5 vol % recrystallized calcite grains that have diameters of ~2.5–7.5 μm. Recrystallized calcite crystals that are twinned typically have a lower density of twins (spaced 5–10 μm apart) than deformed, unrecrystallized grains.

At 600°C, twinning and dislocation glide were still prevalent, but microstructures indicative of dynamic recovery and dynamic recrystallization also are found. All samples show microstructural evidence of recovery in the form of subgrains. Samples strained at rates of 10^{-6} and 10^{-7} s^{-1} that did not form aragonite, contain 10–20 vol % of 5–50 μm diameter subequant calcite neoblasts along deformed calcite grain boundaries (Fig. 3c). The result is a 'core-and-mantle' texture similar to that described for deformation 'Regime 2' of Carrara marble by Schmid *et al.* (1980)—although their samples were coarser grained (200 μm) and deformed at higher temperatures (700–1000°C) and faster strain rates

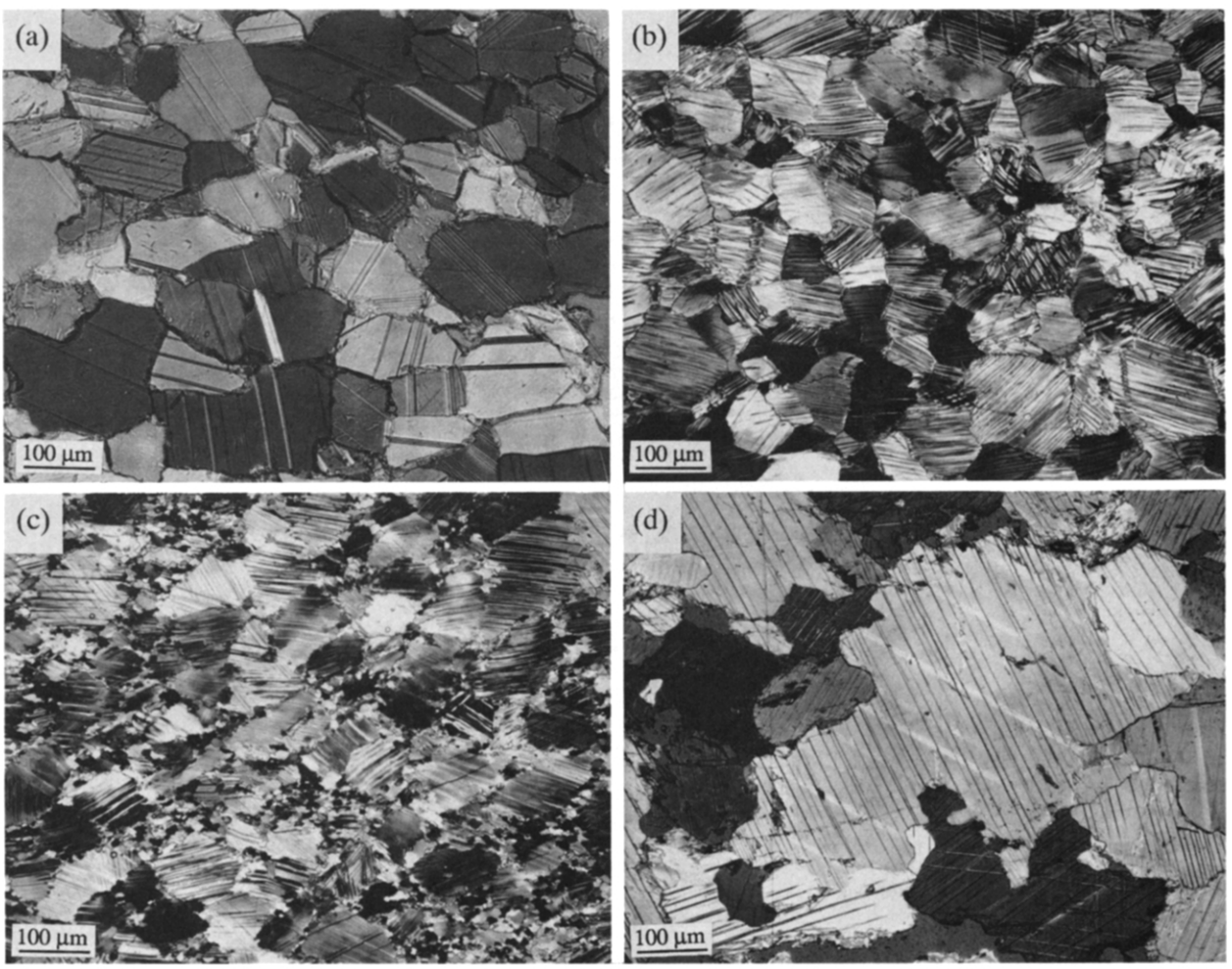

Fig. 3. Optical microstructures of undeformed and deformed Carrara marble photographed with partially crossed polarized light. All photographs have the same 100 μm scale bar. Deformed samples were shortened parallel to the short dimension of the photographs. (a) Carrara marble starting material. Grain size is ~78 μm. (b) Deformation twinning and dislocation glide dominate at 400°C (sample N708 strained 27% in 6 h at 10^{-5} s^{-1}, 400°C, 1.50 GPa and a flow stress of 502 MPa). Most twin boundaries are subperpendicular to the compression direction. (c) Strain-free calcite neoblasts form by subgrain rotation and grain-boundary migration at 600°C (sample N710 strained 20% in 4 h at 10^{-5} s^{-1}, 600°C, 1.53 GPa and a flow stress of 281 MPa). (d) Grain growth dominates sample microstructure at 800–900°C (sample N766 strained 10% in 4.2 h at 10^{-5} s^{-1}, 900°C, a flow stress of 98–136 MPa and three different confining pressures of 0.5, 1.0 and 1.50 GPa).

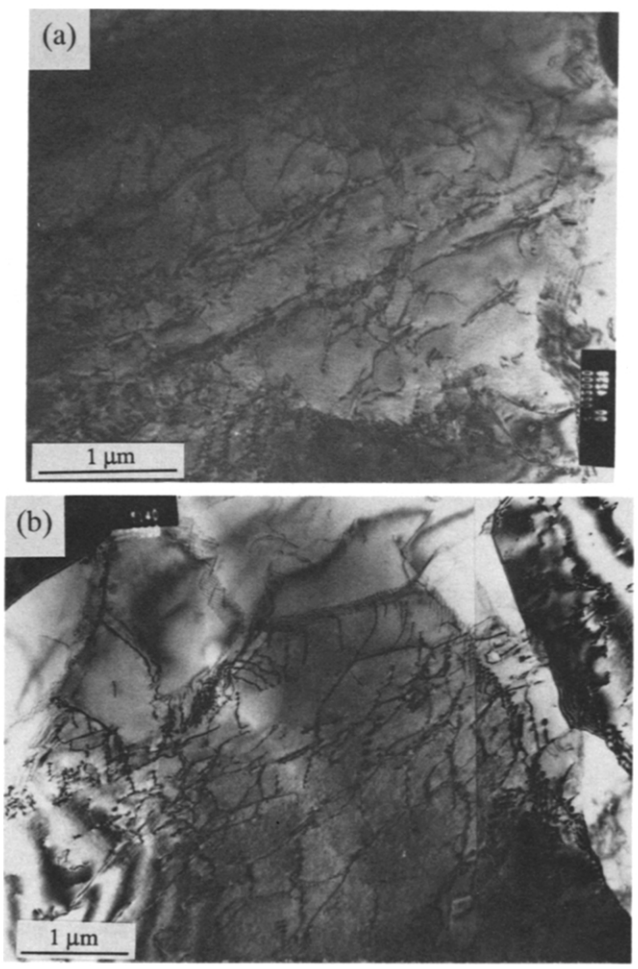

Fig. 4. Representative transmission-electron micrographs of Carrara marble deformed at different confining pressures at 600°C. (a) Sample KP143 strained 8% in 18.5 h at 10^{-6} s^{-1}, 598°C, 0.30 GPa and a flow stress of 54 MPa, in a gas apparatus. (b) Sample N718 strained 29% in 53 h at 10^{-6} s^{-1}, 600°C, 1.54 GPa and a flow stress of 176 MPa, in a solid-medium apparatus. Note similarities in the dislocation microstructures.

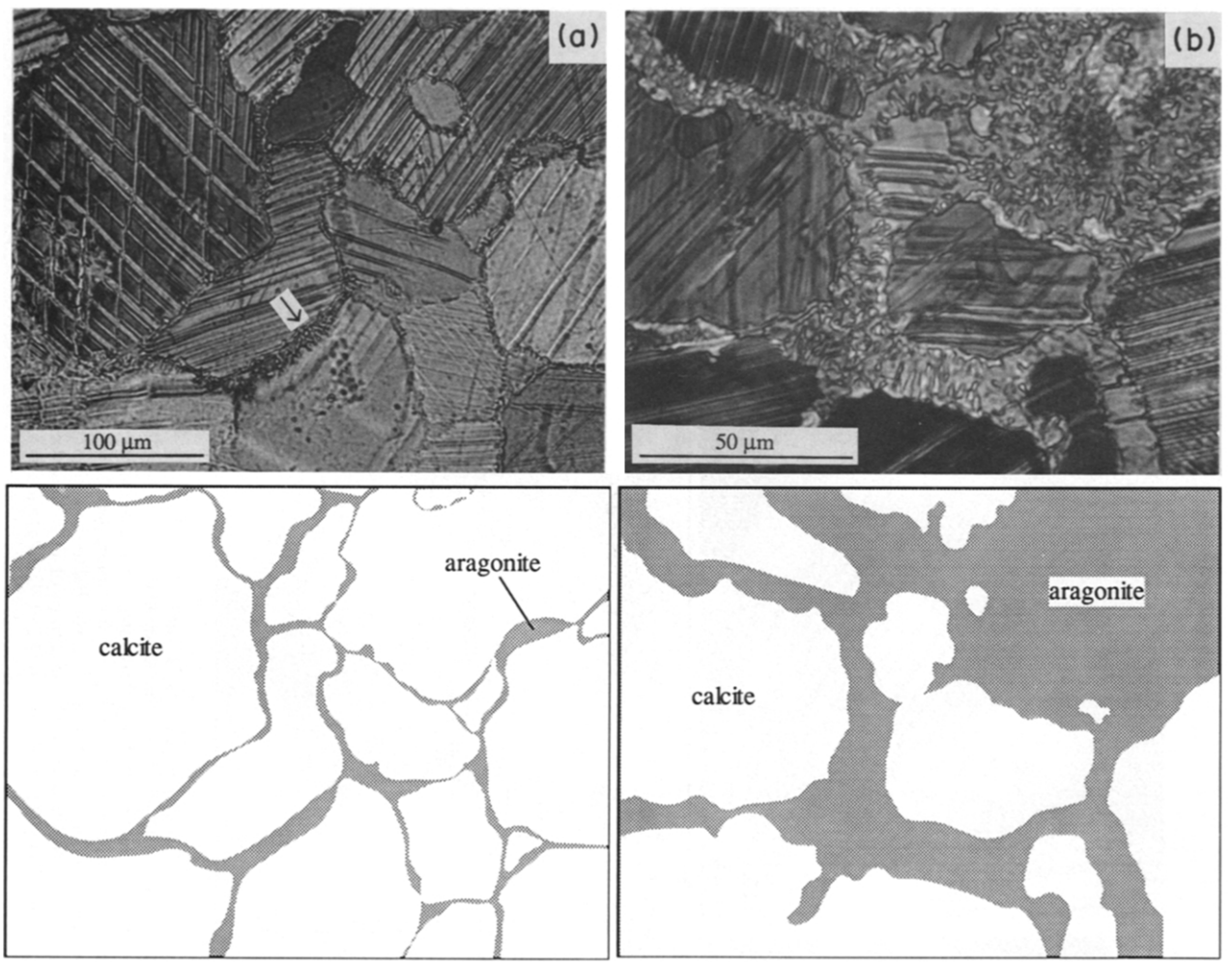

Fig. 5. Growth of aragonite. (a) Initial nucleation along calcite–calcite grain boundaries in sample N738 strained 5% in 21 h at 10^{-6} s^{-1}, 600°C, 1.98 GPa and a flow stress of 243 MPa. Compression direction was parallel to short dimension of photograph. Arrow denotes the area of greatest transformation. (b) About 20% aragonite formed along calcite grain boundaries in sample N719 strained 18% in 67 h at 10^{-6} s^{-1}, 600°C, 1.92 GPa and a flow stress of 203 MPa. Compression direction was parallel to short dimension of photograph.

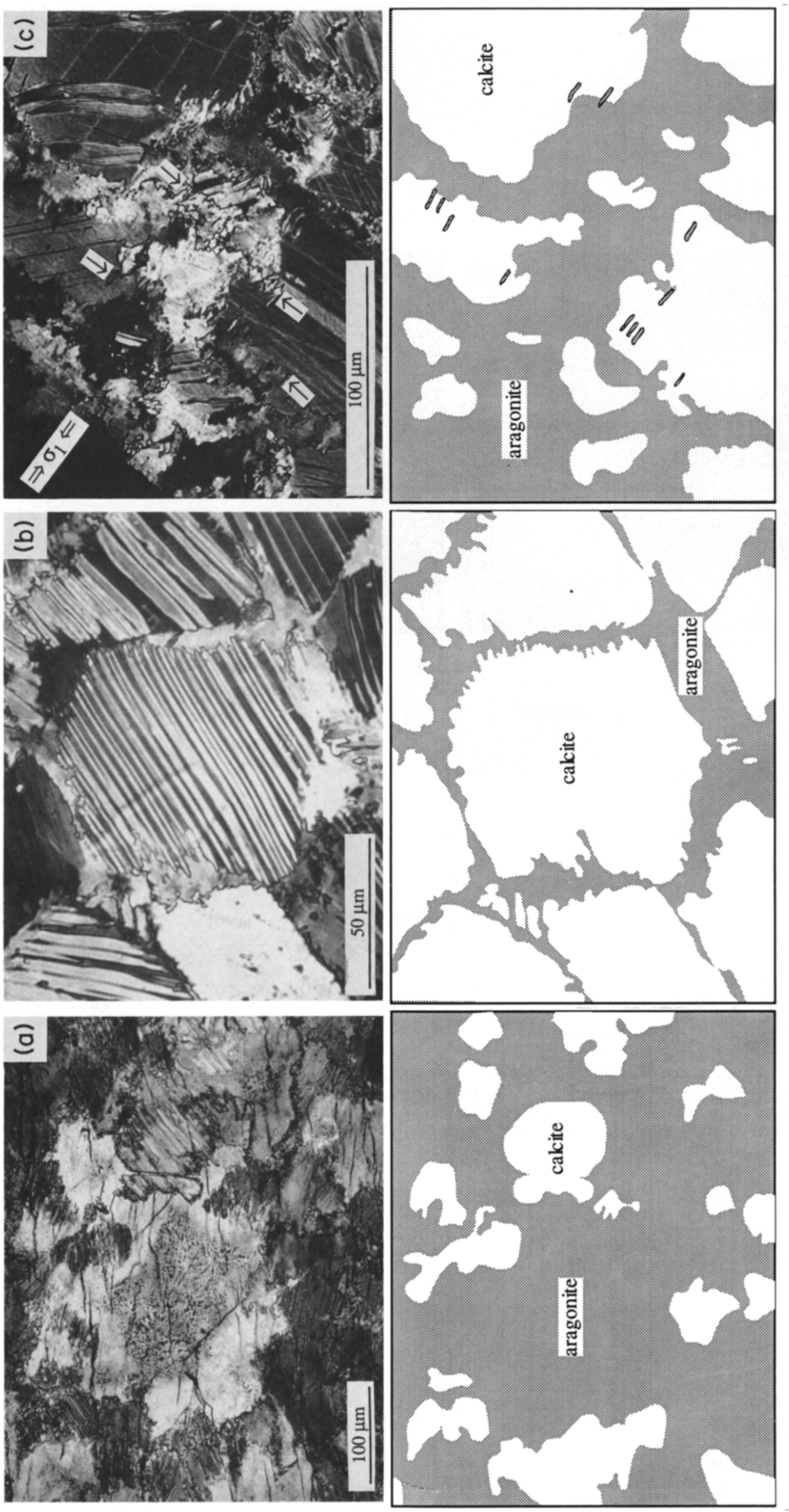

Fig. 6. (a) Aragonite porphyroblasts formed in sample N737 strained 21% in 72 h at 10^{-6} s^{-1}, 500°C, 1.99 GPa and a flow stress of 281 MPa. Twins in relict calcite crystals are easily visible. Clouded centers of aragonite grains may contain small relict or recrystallized calcite(?) crystals. Compression direction was parallel to short dimension of photograph. (b) Growing aragonite crystals preferentially consumed twinned portions of host calcite crystals. The anisotropy of aragonite crystal shape may be driven by local differences in free energy related to deformation. Sample N737 strained 21% in 72 h at 10^{-6} s^{-1}, 500°C, 1.99 GPa and a flow stress of 281 MPa. (c) In one sample, growth of aragonite was greatest parallel to the applied compression direction. Elongate aragonite crystals shown by single arrows, compression direction shown by double arrows. The anisotropy of aragonite crystal shape may be driven by the imposed stress field. Sample N719 strained 18% in 67 h at 10^{-6} s^{-1}, 600°C, 1.92 GPa, and a flow stress of 203 MPa.

(mostly 10^{-3}–10^{-5} s^{-1}). Relict grains in our samples contain twins, undulatory extinction and elongate subgrains, whereas the recrystallized grains are equiaxed to slightly oblate and variably twinned. Areas of advanced dynamic recrystallization comprise grains with straight edges and 60° triple junctions. TEM reveals abundant evidence of climb in the form of curved unit dislocations, dislocation triple junctions and prismatic loops (Fig. 4). The densities of dislocations not in tangles or subgrain boundaries range from 10^{12} to 10^{13} m^{-2}. Subgrain boundaries are also present. Microcracks are rare and those that are present may be related to depressurization and cooling at the end of the experiments. There is no marked difference in TEM-scale deformation microstructures produced at 0.3 GPa and 1.5 GPa confining pressure at 600°C (Fig. 4).

Recrystallization occurred in about half the volume of the two samples strained 3–4% at 700°C and 10^{-5} s^{-1} strain rate. The recrystallized grains that were restricted to host grain boundary regions at lower temperatures, have at 700°C subdivided entire host grains into 10–30 μm grains. The sample tested at 800°C consists mostly of 50–70 μm diameter recrystallized grains and a smaller volume (~15%) of grains as large as 400 μm. Strongly twinned and bent crystals are less abundant than at lower temperatures. Schmid *et al.* (1980) noted similar recrystallization in their Carrara marble deformation 'Regime 3'—although, again, their samples were deformed at higher temperatures (1000°C) to smaller strains (~10%) and were coarser grained. By 900°C, many grains in our samples had grown to 400 μm in diameter, significantly larger than the starting material, indicating that grain boundary mobility increases steeply with increasing temperature (Fig. 3d). This exaggerated or secondary grain growth was found by Schmid *et al.* (1980) in their Carrara marble samples tested at 1000°C. Schmid *et al.* (1980) also found a correlation between recrystallized grain size and stress in their Regimes 2 and 3. Our limited number of experiments at 600–700°C show a similar inverse relationship between grain size and stress.

Aragonite

Hacker *et al.* (1992) found that under hydrostatic pressure oversteps of 0.1–1.0 GPa, nucleation of aragonite in marble occurred very rapidly and that the rate of the transformation was dominated by the rate of aragonite growth, rather than being limited by nucleation rate. At temperatures of 600–750°C, aragonite formed an intergrowth with calcite similar in appearance to cellular precipitation microstructures (e.g. Porter & Easterling 1981, p. 325). Micron-scale finger-shaped inclusions within the aragonite are inferred to be calcite based on optical continuity with nearby relict calcite crystals. At 800°C, subhedral to euhedral aragonite neoblasts without included calcite fingers formed on grain boundaries.

Different habits of aragonite formed at different rates in our Carrara marble samples deformed within the aragonite stability field (Fig. 1). Aragonite is found only in samples tested for long durations (18–524 h, corresponding to strain rates of 10^{-6} and 10^{-7} s^{-1}), and is most abundant in samples tested in relatively high temperatures (600°C) and confining pressures (1.7–2.0 GPa). It is apparent from Fig. 1 that pressure oversteps of ~0.5 GPa and experiment durations of >1 h are required for aragonite growth in our 600°C experiments, whereas experiments longer than 50 h are needed at 500°C. One sample tested for 68 h at 700°C and a pressure nominally within the aragonite stability field did not transform to aragonite. Given the rapid transformation rate observed at 600°C, this result suggests that the pressure on the sample was at least 0.18 GPa (9%) less than the gauge pressure. Two samples also contain aragonite only near the piston at one end of the sample. One of these samples (N748) was deformed at 2.0 GPa and 600°C, a pressure and temperature at which aragonite was produced in samples tested at slower strain rates (10^{-6} rather than 10^{-4} s^{-1}), and the other sample (N749) was deformed 18 h longer than any other sample tested at 2.0 GPa and 400°C.

Aragonite neoblasts that formed in Carrara marble deformed at 600°C are similar to those grown in hydrostatic experiments at 600–700°C. Specifically, the aragonite crystals contain fingers about 1 μm wide that we infer to be calcite (Fig. 5a). These calcite(?) fingers were apparently included during aragonite growth. In more extensively transformed samples, the aragonite crystals formed large domains of tightly packed grains. Groups of these grains have similar, but measurably different, orientations. Remnant calcite crystals within areas almost completely transformed to aragonite have dentate grain boundaries with narrow relict arms pointing into the advancing aragonite (Fig. 5a). At 600°C and 2.0 GPa, aragonite crystals grew at a rate of $6 \pm 2 \times 10^{-11}$ m s^{-1} (Fig. 7a), producing grains ranging in size from a few to ~70 μm. The amount of aragonite formed in samples at 600°C and 2.0 GPa varies with time in a manner shown in Fig. 7(b).

At 500°C, aragonite grows in a habit that has not been found in samples hydrostatically heated at 500–800°C or in samples deformed at temperatures of 400 or 600°C (Fig. 6a). These unusual aragonite crystals are large, 100–200 μm in diameter, porphyroblastic, and are composed of many slightly misoriented subgrains. They are found in conjunction with 'normal' smaller aragonite neoblasts and are not homogeneously distributed throughout samples in which they occur. The porphyroblasts appear to have nucleated on grain boundaries and then grown by rapid consumption of multiple, whole calcite crystals. The diameters of these grains and the durations of the experiments in which they were produced mandate an average growth rate in excess of 8×10^{-10} m s^{-1}. The apparently accelerated growth rate and the inhomogeneous distribution of the porphyroblasts indicate that the growth mechanism of the porphyroblasts is different from that of aragonite grown at higher temperatures. The aragonite porphyroblasts lack mechanical twins, but typically contain many cracks that are

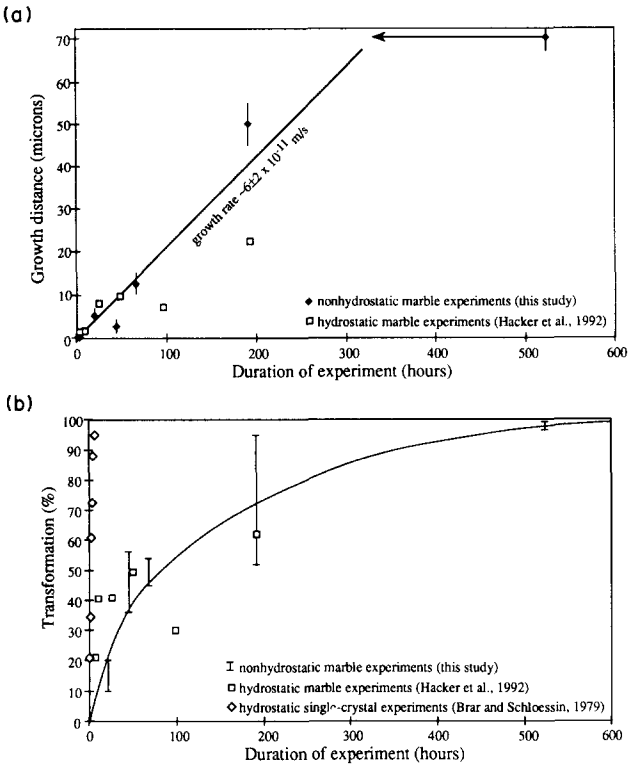

Fig. 7. Growth rate (a) and transformation rate (b) of calcite to aragonite at 600°C and 2.0 GPa vs time. (a) The datum at 524 h is a maximum value because the length of the fingers is essentially equal to the grain size of the starting material; this same growth could have occurred in a shorter time as shown by the arrow. (b) Brackets illustrate the range of transformation encountered along the length of samples as a result of temperature gradients. Data from hydrostatic single crystal (unfilled diamonds; Brar & Schloessin 1979) and marble experiments (filled squares; Hacker *et al.* 1992) are shown for comparison.

orthogonal to the compression direction. These cracks presumably formed during unloading and quenching.

All deformed Carrara marble samples which partially transformed to aragonite include areas where the aragonite crystals grew farther into certain orientations of twinned calcite grains (Fig. 6b). Because the deformation twins are dominantly orthogonal to σ_1 as a result of twinning-induced rotation in response to compression (see above), this preferential growth produced aragonite grains that are elongate parallel to σ_3.

DISCUSSION

Comparison of Carrara marble and Solnhofen limestone

Wenk *et al.* (1973) performed synkinematic calcite →aragonite transformation experiments on Solnhofen limestone, affording the opportunity for comparison with our experiments on Carrara marble. In comparison to Carrara marble, Solnhofen limestone has much smaller (5 μm diameter) grains and more impurities. Talc was used as the confining medium and the samples were not jacketed. Aragonite formed at the ends of Solnhofen samples near pistons within 10 h at 300°C, 1.5 GPa and 10^{-4} s^{-1} strain rate. In contrast, we observed aragonite near pistons in Carrara marble only to temperatures as low as 400°C; no aragonite formed in Carrara marble at confining pressures of 1.5 GPa at any temperature or strain rate—even in runs as long as 27 h. Widespread aragonite formed in Solnhofen limestone in less than 1 h at temperatures as low as 400°C at a confining pressure of 1.0 GPa (Wenk *et al.* 1973), whereas we found bulk transformation in Carrara marble only to temperatures as low as 500°C at 1.7–2.0 GPa—and only in 10^{-6} s^{-1} runs lasting 18–21 h. The greater reactivity observed in Solnhofen limestone at lower temperatures and lower reaction free energies (i.e. lower pressures) may be attributable to two obvious differences between the samples. The Solnhofen samples were encased in a confining medium of talc, which undoubtedly supplied some water to the samples, whereas the Carrara marble samples were vacuum dried and chemically isolated in silver jackets. The fine grain size of the Solnhofen samples should also have promoted more rapid reaction, because (1) smaller grains contribute more grain-boundary free energy per unit volume than larger grains, and (2) the amount of aragonite nucleated in a given time is inversely proportional to grain size for grain-boundary nucleated reactions (Cahn 1956). Further comparison between Solnhofen limestone and Carrara marble is made in the following section.

Aragonite growth morphologies

The present deformation study as well as the hydrostatic experiments of Hacker *et al.* (1992) reveal that, at least in the laboratory, there are three morphological types of aragonite that grow. The most common morphology is that of anhedral ~5–7 μm diameter aragonite 'gloves' that include 'fingers' of what we infer to be calcite. This texture is very similar to cellular precipitation, and has been observed in hydrostatic experiments at 600–750°C and in deformation experiments at 500–600°C.

A different morphology of aragonite, large 100–200 μm porphyroblasts, grew in two samples of Carrara marble deformed at 500°C. These two samples with porphyroblastic aragonite are the only samples in which aragonite formed at 500°C; both were shortened >20% at 10^{-6} s^{-1} strain rate. These grains grew about one order of magnitude faster than aragonite grew at 600°C. The accelerated growth rate suggests that the growth mechanism is different. It is probable that the more heavily deformed and less recovered calcite grains in our samples tested at 500°C had larger defect free energies than calcite grains in samples deformed at 600°C, and thus provided an additional energy source for aragonite growth. Snow & Yund (1987) reported that calcite crystals growing in an aragonite host polycrystal (i.e. the reverse reaction of this study) were unable to penetrate aragonite–aragonite grain boundaries, because the high-angle boundaries interrupted the aragonite substrate on which the calcite grew. This explanation does not obtain for the reverse reaction in our samples, because the porphyroblastic aragonite crystals consumed multiple

Table 1. Estimated free energies of defects in deformed marble*

	Coherent twins	Grain boundaries	Dislocations
Linear/areal free energy(Jm^{-2})	2.3×10^{-3}	7×10^{-2}	7×10^{-9}
Density (m^{-1})	10^5	8.6×10^4	10^{13}
Volume free energy ($J\ mol^{-1}$)	0.085	0.222	2.6

*Computed using 3.693×10^{-5} $m^3\ mol^{-1}$ for the molar volume of calcite (Holland & Powell 1985).

calcite grains. Wenk *et al.* (1973) have also reported anomalously large porphyroblastic aragonite crystals (1–8 mm in diameter) in two samples of Solnhofen limestone. However, their samples were deformed at 1.47 GPa and 600°C at 10^{-6} s^{-1}, and 2.2 GPa and 800°C at 10^{-5} s^{-1}, temperatures at which dynamic recrystallization should have operated. Wenk *et al.* (1973) attributed the porphyroblastic aragonite habit to slow nucleation rates near the calcite–aragonite equilibrium boundary. Porphyroblasts occur in our Carrara marble samples tested relatively far from the equilibrium boundary, suggesting that some other factor controls the appearance of aragonite porphyroblasts.

A third type of aragonite morphology occurred in hydrostatic tests at 800°C where equant, sub- to euhedral aragonite grains grew along original calcite–calcite grain boundaries (Hacker *et al.* 1992). We conducted no corresponding deformation tests at 800°C because the pressure required for aragonite stability at that temperature exceeds the safe range of our apparatus (Fig. 1).

Effects of stress and deformation on the transformation

Transformations can be affected by stress and deformation, and the present experiments provide the opportunity to assess this posibility for calcite→aragonite. The assessment may not be particularly apt because the deformation and hydrostatic experiments were conducted in similar but somewhat different apparatus, however, the deformation experiments differ from the hydrostatic experiments in only the following rather insignificant ways: (1) the temperature is measured at the side of the sample instead of at the top; (2) the pressure is applied by two coaxial pistons rather than one; and (3) each sample is sandwiched between two ceramic end pieces rather than by NaCl and MgO.

Glovelike aragonite crystals grew at a rate of $6 \pm 2 \times 10^{-11}$ m s^{-1} in the present deformation experiments, a rate that is not significantly different from the rate at which aragonite crystals grew in hydrostatically treated samples under similar pressures and temperatures ($7–10 \times 10^{-11}$ m s^{-1}; Hacker *et al.* 1992). This suggests that stress and deformation do not appreciably affect these rates at our experimental conditions.

Deformation-induced effects on transformation. The free energy of a defect (grain boundary, twin, dislocation, etc.) can aid in nucleation and growth if the neoblast can accommodate some of the free energy of the defect. What contribution do these energy sources make in comparison to reaction free energy? The free energies of defects in calcite can be estimated by calculation and by comparison to metals. The free energy of a dislocation can be approximated as:

$$\Delta G_d = Kb^2 \ln\left(\frac{R}{r_0}\right) + \alpha K b^2,$$

where K is an energy factor that depends on the geometry of the dislocation and the elastic constants of the material, b is the magnitude of the Burgers vector (between 0.5 and 1.7 nm in calcite), R is the radius of the strain field around the dislocation, r_0 is the dislocation core radius and α is a constant (Heinisch *et al.* 1975; Wintsch & Dunning, 1985). Following Wintsch & Dunning (1985), we take $\alpha = 0.3$, $r_0 = b$, and $R = 1/(2\sqrt{\rho})$, where ρ is the dislocation density. For the dislocation densities of 10^{12}–10^{13} m^{-2} we observed in Carrara marble deformed at 600°C, the linear free energies are $\sim 7 \times 10^{-10}$ J m^{-1} for $b = 0.5$ nm and $\sim 7 \times 10^{-8}$ J m^{-1} for $b = 1.7$ nm. The volume free energy contributed by dislocations is $\Delta G_d V \rho$. For a 10^{13} m^{-2} density of $b = 0.5$ nm dislocations, this free energy contribution is 2.6 J mol^{-1} (assuming the molar volume of calcite is $V = 3.693 \times 10^{-5}$ m^3 mol^{-1}; Holland & Powell 1985).

The only measurement of interfacial free energy in calcite, to our knowledge, is the cleavage free energy measurements of Gilman (1960). Gilman (1960) measured the free energy of the $\{10\bar{1}0\}$ surface of calcite as 0.23 J m^{-2}. In many cubic metals, the ratios of surface free energy to grain-boundary free energy to coherent twin free energy are in the neighborhood of 1.00:0.30:0.01 (Murr 1975). Assuming that the same interfacial free energy ratios obtain for calcite, the free energies of calcite grain boundaries and coherent twins are estimated to be in the vicinity of 0.07 and 0.0023 J m^{-2}, respectively. For Carrara marble of 78 μm grain size, assuming that the ratio of grain-boundary area to volume is 6.7, the grain-boundary free energy is ~0.222 J mol^{-1}. For the twin spacings of 1–10 μm that we observed in our deformed samples (Table 1), this implies free energy contributions of ~0.085–0.0085 J mol^{-1}.

Note that for this study, these calculations suggest that finely spaced twins contribute the same order of magnitude of free energy as the grain boundaries. The volume free energy change of calcite→aragonite is about −1500 J mol^{-1} at the experimental conditions of 600°C and 2.0 GPa (about 0.5 GPa into the stability field of aragonite). In other words, at those conditions the volume free energy dominates any possible free-energy contribution from defects, so that the stability of calcite relative to

aragonite will not be appreciably influenced by the density of dislocations and twins observed in our experimentally deformed marble. The free energy contribution of defects should be important only in situations where: (1) the defect density is several orders of magnitude higher; or (2) the transformation is occurring under conditions closer to equilibrium such that the volume free energy of the reaction is lower. The latter, near-equilibrium conditions could result from externally imposed pressure and temperature or from internal changes in pressure caused by the volume change of reaction.

Samples partially transformed to aragonite include areas where the aragonite crystals grew farther into certain orientations of twinned calcite grains (Fig. 6b). Because the deformation twins are dominantly orthogonal to σ_1 as a result of twinning-induced rotation in response to compression, this preferential growth produced aragonite grains that are elongate parallel to σ_3. No anisotropic aragonite growth of this type has been observed in hydrostatically transformed samples because of the paucity of twinning in those samples (Hacker *et al.* 1992).

Stress-induced effects on transformation. Previous studies have shown that differential stress can cause anisotropic grain growth and we have observed some effects of this in deformed Carrara marble. Vaughan *et al.* (1984) found for the Mg_2GeO_4 olivine→spinel transformation that spinel nucleated preferentially on boundaries normal to σ_1, and grew faster parallel to σ_1. Consequently, the residual olivine porphyroclasts became elongate normal to the compression direction, regardless of the orientation of the host olivine crystals. The spinel grew as fingers 1–5 μm across and up to 10 μm long that pointed into the olivine. Vaughan *et al.* (1984) proposed that the rate at which an interface grows is influenced by the imposed stress field. Their formulation implies that the stability of a phase depends not only on pressure and temperature, but also on the orientation of interphase boundaries in relation to the stress field; the higher the normal stress on an interface, the greater the driving potential, and presumably, the higher the growth rate. They assumed that the state of stress on the bounding surface of a nucleus conforms to that of the applied stress. They calculated that near the equilibrium boundary, the growth rate of an interface would be markedly anisotropic for a reaction involving a volume change.

In most deformed Carrara marble samples containing aragonite, the aragonite crystals were found to have penetrated into calcite crystals ~2–5 μm farther in the direction parallel to the compression axis, σ_1 (Fig. 6c). The anisotropic aragonite growth occurred only locally in samples, and never on the scale observed by Vaughan *et al.* (1984). This suggests that the theory proposed by Vaughan *et al.* (1984) is not generally applicable to polymorphic mineral transformations.

Green & Burnley (1989) and Burnley *et al.* (1991) later conducted a more comprehensive deformation study of the orthogermanate system and found that the olivine polymorph could exist metastably in the spinel field at temperatures of about 1423–1523°C when shortened at strain rates exceeding 10^{-4} s^{-1}. Spinel inclusions formed in their samples were quite different from those of Vaughan *et al.* (1984): they were lens shaped with long axes perpendicular to the compression direction. Green & Burnley (1989) hypothesized that the state of stress around the spinel inclusions was altered by the strength of spinel, which they suggested was significantly weaker than olivine due to superplastic deformation. Using an analogy of the stress field around a crack, they reasoned that the axial stress was highest in inclusion boundaries parallel to the compression direction and that consequently the driving potential and spinel growth rates were greatest in the direction normal to the compression direction. Similar inclusion morphologies were observed in H_2O ice I samples deformed while transforming to ice II (Kirby *et al.* 1991). In the present experiments we have not observed lens-shaped inclusions of aragonite of the type described above. Several contrasts in the transformation microstructures and experimental conditions are noteworthy. First, the aragonite grains nucleated on grain boundaries and are generally coarser than spinel produced in the orthogermanate. Thus there is no reason to suspect that aragonite was weak because of ultrafine grain size—a necessary condition for the stress redistribution around lens-shaped inclusions. Second, the differential stress in the present experiments was smaller in relation to the confining pressures and equilibrium pressures, meaning that the normal stress anisotropy and hence anisotropy in driving potential for transformation was far smaller. Third, all the experiments on orthogermanate and ice I involved shortening rates faster than 10^{-4} s^{-1}, whereas aragonite only formed at strain rates of 10^{-5} s^{-1} or less and mostly 10^{-6} s^{-1} or less. This may be significant if latent heat enhances transformation in short experiments where such heat cannot conduct away from the inclusions fast enough. This hypothesis might be tested by conducting higher strain rate tests on calcite or lower strain rate experiments on ice or orthogermanate.

Rheological effects of the transformation

Phase transformations can affect the rheology of materials in a number of ways. For example, the product phase may have mechanical properties notably different from the reactant phase, or the linear transformation strain, $\approx(\Delta V/V_o)/3$, may accommodate some of the axial strain. We find for Carrara marble that samples containing aragonite are not systematically stronger or weaker than samples lacking aragonite (Fig. 8). The scatter and uncertainties of the strength measurements, combined with the necessity of comparing strengths measured at different strain rates, renders this comparison rather qualitative. Gillet *et al.* (1987) claimed that marble samples they transformed experimentally to aragonite were stronger than untransformed marble, but they did not provide details.

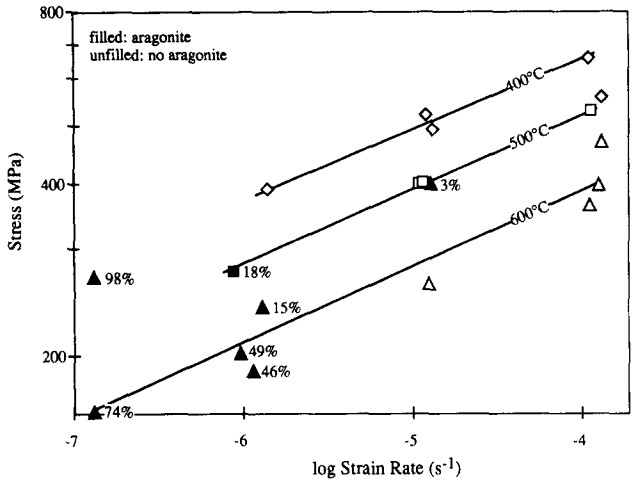

Fig. 8. Strength trends of samples containing aragonite (filled symbols) are not systematically stronger or weaker than strength trends of samples lacking aragonite (unfilled symbols). Percentages indicate average amount of aragonite present.

Lack of shear instability

Many earthquakes occur at depths below where ordinary brittle fracture and frictional sliding are considered to occur. It has been proposed that such deep earthquakes may be the result of mechanical instability occurring during densification phase transformations (Griggs & Handin 1960, Griggs & Baker 1969, Kirby 1987, Green & Burnley 1989, Kirby *et al.* 1991). A shear instability called 'transformational faulting' does occur under non-hydrostatic stress in some compounds undergoing reconstructive transformations, notably tremolite →amorphous phase (Burnley & Kirby 1982), ice I→II (Durham *et al.* 1983, Kirby 1987, Kirby *et al.* 1991), and germanate olivine→spinel (Green & Burnley 1989). Catastrophic failure occurs in samples of ice I or olivine that are loaded outside their stability field at conditions where the transformation rate to the denser phase cannot keep pace with the imposed deformation rate. The volume change of the transformation is important in identifying phase transformations that might undergo transformational faulting; large differences in density between the reactant and product phases increase the likelihood of heterogeneous unstable deformation during transformation. Likewise, the latent heat of reaction may also influence whether a particular phase transformation will lead to catastrophic failure (Kirby 1987, Kirby *et al.* 1991). If the reaction is exothermic and the volume free energy of the product phase decreases with increasing temperature, then transformational faulting is favored. Kirby *et al.* (1991) have proposed that the volume change and latent heat of the calcite→aragonite transformation are too small to promote transformational faulting.

The present study and that of Wenk *et al.* (1973) support this prediction. A shear instability did not develop during the growth of aragonite in any of our Carrara marble samples in spite of the wide range of investigated P–T–σ conditions at which calcite was metastable, and transformation varied from nonexistent to the rapid growth of large aragonite porphyroblasts. Similarly, no general faulting instability associated with coesite formation was observed in an extensive suite of high-pressure quartzite experiments conducted by Tullis (1971) and cited by Griggs (1972), even though the volume change and latent heat of α-quartz→coesite is similar to calcite→aragonite.

CONCLUSIONS

Deformation experiments were conducted on Carrara marble in the aragonite and calcite stability fields at temperatures of 400–900°C, strain rates of 10^{-7}–10^{-4} s^{-1}, confining pressures of 0.1–2.0 GPa and at stresses as high as 660 MPa. At 400–500°C, virtually all calcite plastic deformation occurred by mechanical twinning, whereas rapid recovery occurred and abundant recrystallized grains formed at grain boundaries at 600–700°C. By 900°C, many calcite grains grew significantly larger than the starting material.

Aragonite grew in our 10^{-6}–10^{-7} s^{-1} strain rate tests at confining pressures of 1.7–2.0 GPa in the aragonite stability field. Samples containing aragonite are not systematically stronger or weaker than samples lacking aragonite. Aragonite formed at much lower pressures and temperatures in a similar study by Wenk *et al.* (1973), probably because their Solnhofen limestone samples were much finer grained and enclosed in talc. At 600°C, the growth of aragonite neoblasts produced 'glove-and-finger' textures identical to those observed in our previous hydrostatic experiments. At 500°C, porphyroblastic 100–200 μm aragonite crystals grew almost an order of magnitude faster. Locally, aragonite crystals consumed calcite grains preferentially along twins, resulting in aragonite grains that are elongate orthogonal to the compression axis. In one sample, aragonite crystals were found to have penetrated farther into calcite parallel to the compression axis, σ_1

Aragonite formation is not accompanied by a shear instability, consistent with the relatively small volume change and latent heat of the reaction.

Acknowledgements—John Christie started both of us down the paths that led to this collaboration. John Pinkston assisted ably in the laboratory. Helpful reviews were provided by Ernie Rutter, Laura Stern and an anonymous referee, and Jan Tullis penned particularly in-depth comments. To all we extend our sincere thanks.

REFERENCES

Adams, F. D. & Nicholson, J. T. 1901. An experimental investigation into the flow of marble. *Phil. Trans. R. Soc. Lond.* **A195**, 363–401.

Brar, N. S. & Schloessin, H. H. 1979. Effects of pressure, temperature, and grain size on the kinetics of the calcite→aragonite transformation. *Can. J. Earth Sci.* **16**, 1402–1418.

Burnley, P. C., Green, H. W., II & Prior, D. J. 1991. Faulting associated with the olivine to spinel transformation in $Mg_2GeO_4$and its implications for deep-focus earthquakes. *J. geophys. Res.* **96**, 425–443.

Burnley, P. C. & Kirby, S. H. 1982. Pressure-induced embrittlement of polycrystalline tremolite $Ca_2Mg_5Si_8O_{22}(OH,F)_2$. *Eos* **63**, 1095.

Cahn, J. W. 1956. The kinetics of grain-boundary nucleated reactions. *Acta metall.* **4**, 449–459.

Carlson, W. D. & Rosenfeld, J. L. 1981. Optical determination of topotactic aragonite-calcite growth kinetics: metamorphic implications. *J. Geol.* **89**, 615–638.

Casey, M., Rutter, E. H., Schmid, S. M., Siddans, A. W. B. & Whalley, J. S. 1978. Texture development in experimentally deformed calcite rocks. *5th Int. Conf. Textures of Materials* **2**, 231–240.

Durham, W. B., Heard, H. C. & Kirby, S. H. 1983. Experimental deformation of polycrystalline H_2O ice at high pressure and low temperature; preliminary results, *J. geophys. Res.* **88**, 377–392.

Ferreira, M. P. & Turner, F. J. 1964. Microscopic structure and fabric of Yule marble experimentally deformed at different strain rates. *J. Geol.* **72**, 861–875.

Friedman, M. & Higgs, N. 1981. Calcite fabrics in experimental shear zones. In: *Mechanical Behavior of Crustal Rocks. Am. Geophys. Un. Geophys. Monogr.* **24**, 11–27.

Gillet, P., Gerard, Y. & Williame, C. 1987. The calcite-aragonite transition: mechanism and microstructures induced by the transformation stress and strain. *Bull. Mineral.* **110**, 481–496.

Gilman, J. J. 1960. Direct measurements of the surface energies of crystals. *J. appl. Phys.* **31**, 2208–2218.

Green, H. W., II & Burnley, P. C. 1989. A new self-organizing, mechanism for deep-focus earthquakes. *Nature* **341**, 733–737.

Griggs, D. T. 1967. Hydrolytic weakening of quartz and other silicates. *Geophys. J. R. astr. Soc.* **14**, 19–31.

Griggs, D. T. 1972. The sinking lithosphere and the focal mechanism of deep earthquakes. In: *The Nature of the Solid Earth* (edited by Robertson, E. C.). McGraw Hill, New York, 361–384.

Griggs, D. T. & Baker, D. 1969. The origin of deep-focus earthquakes. In: *Properties of Matter under Unusual Conditions* (edited by Mark, H. & Fernback, S.). Wiley Interscience, New York, 23–42.

Griggs, D. T. & Handin, J. 1960. Observations on fracture and a hypothesis of earthquakes. In: *Rock Deformation* (edited by Griggs, D. & Handin, J.). *Mem. geol. Soc. Am.* **79**, 347–363.

Griggs, D. T. & Miller, W. B. 1961. Deformation of Yule marble: Part I—Compression and extension experiments on dry Yule marble at 10,000 atmospheres confining pressure, room temperature. *Bull. geol. Soc. Am.* **62**, 853–682.

Griggs, D. T., Turner, F. J. & Heard, H. 1960. Deformation of rocks at 500° to 800°C. In: *Rock Deformation* (edited by Griggs, D. & Handin, J.). *Mem. geol. Soc. Am.* **79**, 39–104.

Hacker, B. R., Kirby, S. H. & Bohlen, S. R. 1992. Time and metamorphic petrology: Calcite to aragonite experiments. *Science* **258**, 110–112.

Heard, H. C. 1960. Transition from brittle fracture to ductile flow in Solenhofen limestone as a function of temperature, confining pressure, and interstitial fluid pressure. In: *Rock Deformation* (edited by Griggs, D. & Handin, J.). *Mem. geol. Soc. Am.* **79**, 193–226.

Heard, H. C. 1963. Effect of large changes in strain rate in the experimental deformation of Yule marble. *J. Geol.* **71**, 162–195.

Heard, H. C. & Raleigh, C. B. 1972. Steady-state flow in marble at 500° to 800°C. *Bull. geol. Soc. Am.* **83**, 935–956.

Heinisch, H. L., Jr, Sines, G., Goodman, J. W. & Kirby, S. H. 1975. Elastic stresses and self-energies of dislocations of arbitrary orientation in anisotropic media: olivine, orthopyroxene, calcite, and quartz. *J. geophys. Res.* **80**, 1885–1896.

Holland, T. J. B. & Powell, R. 1985. An internally consistent thermodynamic dataset with uncertainties and correlations: 2 Data and results. *J. metamorph. Geol.* **3**, 343–370.

Johannes, W. & Puhan, D. 1971. The calcite-aragonite transition, reinvestigated. *Contr. Miner. Petrol.* **31**, 28–38.

Kirby, S. H. 1987. Localized polymorphic phase transitions in high-pressure faults and applications to the physical mechanism of deep earthquakes. *J. geophys. Res.* **92**, 13,789–13,800.

Kirby, S. H., Durham, W. B. & Stern, L. A. 1991. Mantle phase changes and deep-earthquake faulting in subducting lithosphere. *Science* **252**, 216–225.

Kronenberg, A. K., Kirby, S. H. & Pinkston, J. 1990. Basal slip and mechanical anisotropy of biotite. *J. geophys. Res.* **95**, 19,257–19,278.

Mirwald, P. W., Getting, I. C. & Kennedy, G. C. 1975. Low-friction cell for piston-cylinder high pressure apparatus. *J. geophys. Res.* **80**, 1519–1525.

Murr, L. E. 1975. *Interfacial Phenomena in Metals and Alloys.* Addison-Wesley, London.

Porter, D. A. & Easterling, K. E. 1981. *Phase Transformations in Metals and Alloys* (1st edn). Chapman and Hall, London.

Rowe, K. J. & Rutter, E. H. 1990. Paleostress estimation using calcite twinning: experimental calibration and application to nature. *J. Struct. Geol.* **12**, 1–17.

Rutter, E. H. 1972. The influence of interstitial water on the rheological behaviour of calcite rocks. *Tectonophysics* **14**, 13–33.

Rutter, E. H. 1974. The influence of temperature, strain rate, and interstitial water in the experimental deformation of calcite rocks. *Tectonophysics* **22**, 311–334.

Schmid, S. M., Boland, J. N. & Paterson, M. S. 1977. Superplastic flow in finegrained limestone. *Tectonophysics* **43**, 257–291.

Schmid, S. M., Paterson, M. S. & Boland, J. N. 1980. High temperature flow and dynamic recrystallization in Carrara marble. *Tectonophysics* **65**, 245–280.

Snow, E. & Yund, R. A. 1987. The effect of ductile deformation on the kinetics and mechanisms of the aragonite–calcite transformation. *J. metamorph. Geol.* **5**, 141–153.

Tullis, J. A. 1971. Preferred orientations in experimentally deformed quartzites. Unpublished Ph.D. thesis, University of California, Los Angeles.

Vaughan, P. J., Green, H. W. & Coe, R. S. 1984. Anisotropic growth in the olivine–spinel phase transformation of Mg_2GeO_4 under nonhydrostatic stress. *Tectonophysics* **108**, 299–322.

von Kármán, Th. 1911. Festigkeitversuche unter allseitigem Druck. *Z. Vereins dt. Ingen.* **55**, 1749–1757.

Weiss, L. E. & Turner, F. J. 1972. Some observations on translation gliding and kinking in experimentally deformed calcite and dolomite. In: *Flow and Fracture of Rocks* (edited by Heard, H. C., Borg, I. Y., Carter, N. L. & Raleigh, C. B.). *Am. Geophys. Un. Geophys. Monogr.* **16**, 95–107.

Wenk, H. R. 1985. Carbonates. In: *Preferred Orientations in Deformed Metals and Rocks: An Introduction to Modern Texture Analysis* (edited by Wenk, H. R.). Academic Press, Orlando, 361–384.

Wenk, H. R., Venkitasubramanyan, C. S. & Baker, D. W. 1973. Preferred orientation in experimentally deformed limestone. *Contr. Miner. Petrol.* **38**, 81–114.

Wintsch, R. P. & Dunning, J. 1985. The effect of dislocation density on the aqueous solubility of quartz and some geologic implications: a theoretical approach. *J. geophys. Res.* **90**, 3649–3657.

APPENDIX

Table A1. Deformation experiments on Carrara marble

Experiment No.	Pressure* (GPa)	Temperature (°C)	Strain rate (s^{-1})	Stress† (MPa)	Strain (%)	Time (h)	Aragonite (%)	Notes
Gas apparatus								
KP142	0.30	405	1.0E−6	180	6.2	24/19	0	
KP141A	0.30	410	1.0E−6	130	1.9	17.6/5.6	0	
KP141B	0.30	403	1.0E−5	155	3.8	1.4/1.1	0	
KP141C	0.30	404	1.0E−4	170	2.7	0.3/0.1	0	
KP155	0.30	398	1.0E−4	200	9	1.2/0.3	0	
KP140A	0.30	507	1.0E−6	95	1.6	19.5/5.5	0	
KP140B	0.30	510	1.0E−5	120	2	12.5/0.9	0	
KP140C	0.30	513	1.0E−4	140	2.5	0.3/0.1	0	
KP143	0.30	598	1.0E−6	54	7.7	17.3/17	0	
KP139A	0.30	600	1.0E−6	63	1.1	5.2/4.2	0	
KP139B	0.30	600	1.0E−5	85	1.6	0.8/0.6	0	
KP139C	0.30	601	1.0E−4	105	5	0.4/0.2	0	
KP156	0.30	600	1.0E−4	130	10	1.5/0.3	0	
KP150	0.50	400	1.0E−6	160	2	9.9/9.6	0	
KP141D	0.50	400	1.0E−5	160	2	2.7/0.7	0	
KP141E	0.50	397	1.0E−4	180	2	0.5/0.4	0	
KP154	0.50	394	1.0E−4	200	9	1.1/0.3	0	
KP144	0.50	498	1.0E−6	64	2	4.45/4.1	0	
KP145A	0.50	510	1.0E−6	95	4	11.2/11	0	
KP145B	0.50	505	1.0E−5	113	2.5	1.1/0.7	0	
KP157	0.50	500	1.0E−5	137	7	3.0/2.0	0	
KP145C	0.50	505	1.0E−4	130	3	0.6/0.3	0	
KP149	0.50	601	1.0E−6	52	8	18.75/18	0	
KP152	0.50	613	1.0E−6	42	8	18/17	0	
KP139D	0.50	600	1.0E−5	85	2	1.8/0.8	0	
KP161	0.10	600	1.0E−5	108	6	2.5/1.25	0	
KP162	0.30	600	1.0E−5	99	8	3.75/2.5	0	
KP159	0.50	600	1.0E−5	80	8.5	6.9/2.3	0	
KP160	0.70	600	1.0E−5	83	4.5	1.6/1.4	0	
KP139E	0.50	597	1.0E−4		3	0.4/0.2	0	
KP153	0.50	600	1.0E−4	125	7	0.95/0.3	0	
Solid-medium apparatus								
N741A	0.33	600	1.6E−7	87	5	138/108	0	
N741B	0.33	600	1.3E−6	97	6.5	24/15	0	
N741C	0.33	600	1.4E−5	149	10	3.5/1.9	0	
N741D	0.33	600	1.4E−4	119	21	0.7/0.4	0	
N764A	0.50	700	1.2E−5	132	3.2	3.3/2.3	0	
N756A	0.53	800	1.3E−5	126	1.7	1.5/0.5	0	
N766A	0.53	900	1.2E−5	98	3.2	1.5/1.0	0	
N750A	1.01	400	1.1E−6	345	3	21/8.6	0	
N750B	1.01	400	1.3E−5	403	5	2.4/1.5	0	
N750C	1.00	400	1.2E−4	514	12	0.5/0.3	0	
N745A	1.01	500	1.2E−6	201	4.3	23/9	0	
N745B	1.01	500	1.2E−5	286	5.6	1.8/1.1	0	
N745C	1.03	500	1.2E−4	345	16	0.4/0.3	0	
N754A	0.99	500	1.2E−6	228	4	24/8.5	0	
N754B	0.99	500	1.3E−5	270	4.4	1.9/1.2	0	
N754C	0.99	500	1.3E−4	337	12	0.5/0.3	0	
N751	0.99	600	1.1E−6	148	23	92/76	0	
N746A	1.02	600	1.3E−5	225	5	1/1	0	
N746B	2.00	600	0.0E+0	0	0	109/0	10	
N753A	1.07	600	1.3E−5	225	4.5	2.4/1.2	0	
N753B	1.07	600	1.3E−4	292	10	0.8/0.2	0	
N755A	1.00	600	1.2E−6	221	2.4	26/22	0	
N755B	1.00	600	1.2E−5	294	4	3.3/2.3	0	
N755C	1.00	600	1.2E−4	294	12	0.7/0.4	0	
N764B	0.98	700	1.3E−5	174	4.3	3/1	0	
N765B	1.00	800	1.2E−5	143	2.5	2.8/0.8	0	
N766B	1.00	900	1.2E−5	109	1.7	0.9/0.5	0	
N756A	1.50	400	1.2E−6	291	3	19/8	0	
N756B	1.50	400	1.2E−5	367	3	3.0/1.8	0	
N756C	1.50	400	1.2E−4	581	3	0.8/0.4	0	
N715	1.53	400	1.0E−6	349	25	72/64	0	
N708	1.50	400	1.1E−5	502	27	6/5	0	
N717	1.48	500	9.5E−7	251	19	67/56	0	
N757A	1.45	500	1.2E−5	368	6	2.2/1.4	0	
N757B	1.48	500	1.2E−4	459	13	0.4/0.3	0	
N718	1.54	600	1.3E−6	176	29	65/53	0	
N710	1.53	600	1.1E−5	281	20	6.0/4.5	0	

continued

Table A1. Continued

Experiment No.	Pressure* (GPa)	Temperature (°C)	Strain rate (s^{-1})	Stress† (MPa)	Strain (%)	Time (h)	Aragonite (%)	Notes
N753C	1.50	600	1.4E−5	270	4	2.8/0.9	0	
N758A	1.49	600	1.2E−5	209	5	2.0/1.1	0	
N758B	1.49	600	1.2E−4	323	9	0.3/0.2	0	
N753D	1.50	600	1.4E−4	298	9	0.1/0.1	0	
N764C	1.51	700	1.2E−5	171	3.4	1.4/0.9	0	
N765C	1.51	800	1.2E−5	155	2.8	2.8/0.8	0	
N766C	1.52	900	1.2E−5	136	5.1	1.5/1.0	0	
N744	1.73	500	7.8E−7	157	36	98/84	15–20	porphyroblastic
N749A	1.99	400	1.4E−6	391	3	2.4/1.5	1 corner	
N749B	2.00	400	1.3E−5	496	6	0.7/0.5	1 corner	
N749C	2.00	400	1.3E−4	567	21	0.5/0.4	1 corner	
N759A	2.01	400	1.2E−5	526	6	0.7/0.5	0	
N759B	1.99	400	1.1E−4	663	21	2.0/1.5	0	
N737	1.99	500	8.7E−7	281	21	72/61	18	porphyroblastic
N747	2.00	500	1.1E−5	399	22	5.5/5.0	0	
N762	2.00	600	1.3E−7	275	20	524/524	97–99	
N763	1.98	600	1.3E−7	160	7.4	192/192	52–95	
N719	1.92	600	9.4E−7	203	18	67/57	45–54	
N736	1.98	600	1.1E−6	189	20	45/35	36–56	
N738	1.98	600	1.3E−6	243	5	21/10	10–20	
N760A	2.01	600	1.2E−5	267	5	5/3	0	
N761A	1.98	600	1.3E−5	399	4	2.7/2.0	0–6	
N761B	2.00	600	1.3E−4	474	15	1.1/0.8	0–6	
N760B	2.00	600	1.2E−4	397	19	0.5/0.4	0	
N748A	2.07	600	1.1E−4	366	9	0.7/0.2	1 corner	
N748B	2.01	500	1.2E−4	459	14	0.6/0.4	1 corner	
N748C	2.00	400	1.3E−4	562	17	0.8/0.6	1 corner	
N742	2.03	700	1.3E−6	170	25	68/40	0	

Experiment numbers with letter suffixes indicate stepping tests. 'Time (h)': total time at pressure/duration of applied differential stress. 'Aragonite (%)': amount of aragonite; range in values encompansses variation from one end of the sample to the other; '1 corner': indicates samples with aragonite developed only in one corner near a piston.

*Strengths reported for samples deformed in solid-medium apparatus are overestimated (see text).

†Pressures reported for samples deformed in solid-medium apparatus are also inaccurate (see text).